Type of the Paper (Article, Review, Communication, etc.)

Optimal Design of Closed-loop Fusion for Sensor Signal Expansion

Yao Mao [1,2,*], Wei Ren [1,2,3], Yong Luo[1,2,3], ZhiJun Li[1,2]

[1] Key Laboratory of Optical Engineering, Chinese Academy of Sciences, Chengdu, 610209, China;
[2] Institute of Optics and Electronics, Chinese Academy of Science, Chengdu, 610209, China;
[3] University of Chinese Academy of Science, Beijing, 100039, China;
* Correspondence: maoyao@ioe.ac.cn; Tel.: +86-155-200-19246

Abstract: Sensor fusion technology is one of extensive used methods in the field of robot, aerospace and target tracking control. In this paper, the generalized sensor fusion framework, named the closed-loop fusion (CLF) is analyzed and the optimal design principle of filter is proposed in detail. Fusion error optimization problem, which is the core issue of fusion design, is also solved better through the feedback compensation law of CLF framework. Differently from conventional methods, the fusion filter of CLF can be optimally designed and the determination of superposition of fusion information is avoided. To show the validity, simulation and experimental results are to be submitted.

Keywords: sensor fusion; fusion error; feedback compensation; closed-loop fusion

---

1. Introduction

Attitude measurement technology of moving objects has been extensively studied by the motion attitude measurement of the robot [1-5], attitude jitter of the satellite [6-9], and other fields []10-11]. A set of reliable and high-precision measurement information for moving attitude is usually obtained by one or multiple sensors. Gyros and accelerometers can sense angular jitter and provide real-time inertial attitude information for moving objects, but inertial sensors produce a continuous error accumulation process due to errors such as drift and noise. To eliminate these errors, a common manner is to first establish sensor models, and then design the Kalman filter based on its drift error propagation mode and noise model, at last combining Kalman filter and another set of sensor to estimate the drift [12-15]. There are for two main problems with this method. One is that the drift error model of the sensor may not be determined. The other is which the data bandwidth is usually limited to a few Hzs in the manner of Kalman. Although it may satisfy the requirement to measure the motion posture of an object, but cannot be adopted to further achieve stable control with high bandwidth [16]. It is currently unrealistic to find a single sensor that not only has small drifts and small noise, but also provides superior measurement bandwidth. However, we believe a realizable way that combining different advantages of two sensors to design a new sensor model with performance better in all frequencies.

The detection ability of sensor in frequency can be easily divided into low bandwidth measurement sensors and high bandwidth measurement sensors [17-18]. Therefore, sensor data onto two different characteristics can be combined in the form of a combined filter. This method is quite simple to use, but the frequency characteristics of the relevant sensors must be known using this method, otherwise we can't design a combination filter to solve the frequency response overlaps problem during the fusion process. In order to surmount the shortcomings of the previous methods, Algrain, M.C proposes an alternative method which is called closed-loop fusion (CLF) [19]. In this method, the measurement data of the low bandwidth sensor and the high bandwidth sensor are adjusted by a closed-loop corrector. Compare to the aforementioned method, it does not require accurate model or transfer function of the sensor, and the drift error of the sensor is also effectively eliminated by the feedback compensation structure. However, he did not point out the reasonable design method of the closed-loop corrector. In the process of experiment, we found that if the characteristics of the closed-loop corrector are designed too soft, the high-pass sensor cannot track the low-pass sensor. On the contrary, if the closed-loop corrector is too hard, the high frequency will influence the low frequency correction term and make the correction invalid. Take into account this problem, we propose optimal design guidance of CLF filter.

In the second part, we will analyze the basic principles of fusion and derive the optimal design of CLF filter. In the third part, the simulation and experimental results will verify the correctness of these design guidelines. The fourth part deals these conclusions.

2. Closed-loop Fusion Framework

In this part, we study the CLF structure and theoretically analyze the optimal fusion design implementation. Our researchers begin with a simple combination fusion principle, and then we propose our own fusion structure based on the basic principles of fusion.

2.1. Basic Principle of Fusion

It is assumed that there are two sensors U_1 and U_2 with inconsistent characteristics, and the two sensors are low-bandwidth property and high-bandwidth property, respectively, and the transfer functions can be defined as G_{low} and G_{high}. In order to obtain a signal with all-pass characteristics over the entire spectrum. The simplest fusion idea is to directly add the two sensors data linearly. However, the simple linear addition processing operation inevitably has signal overlap in the entire frequency band. Figure 1 shows in the process of sensor fusion. The error resulted from the overlap is deviated from the information expressed by the real object.

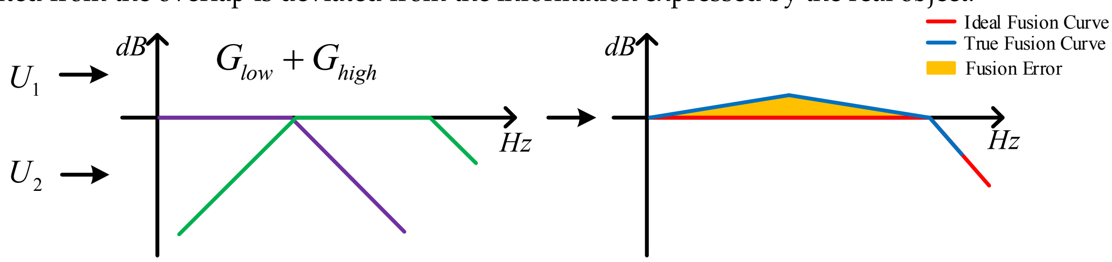

Figure 1. Fusion process of sensor signals in the frequency domain.

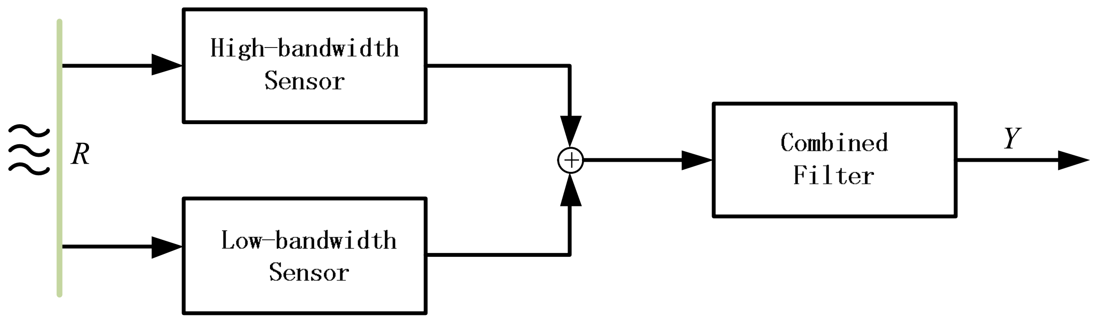

Figure 2. Fusion process of combined filter method.

The traditional approach is that the combined filter method is adopted to eliminate the fusion error by sensor characteristic cancellation in Figure 2. If we know the expressions of G_{low} and

Preprints (www.preprints.org) | NOT PEER-REVIEWED | Posted: 20 November 2018 doi:10.20944/preprints201811.0497.v1

Peer-reviewed version available at *Sensors* **2019**, *19*, 133; doi:10.3390/s19010133

G_{high}, then linear overlap errors can be removed when the combined filter is $\frac{1}{G_{low}+G_{high}}$ in theory [19]. Note that the premise of implementing this method is the fact that we can know or measure the transfer function of the sensor.

2.2. Closed-loop Fusion Scheme

In this section, an advance fusion structure is proposed for fusion technologies. Its advantage is that it does not need to know the sensor property, and conveniently realize the optimal fusion design. The CLF network with real-time correction as shown in Figure 3. G_c represents fusion filter which used to correct the fusion error of two data channels in real time. R is the physical motion quantity, and Y_f is the fusion output.

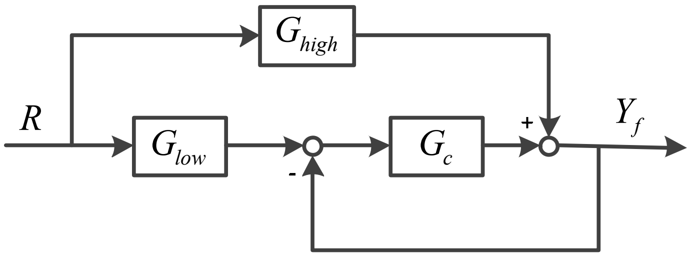

Figure 3. The CLF Scheme.

The transfer function of CLF can be expressed as

$$G_{cl\_fusion} = \frac{Y_f}{R} = \frac{1}{1+G_c} \cdot G_{low} + \frac{G_c}{1+G_c} \cdot G_{high} \tag{1}$$

From the perspective of control, according to the transfer function of CLF, $\frac{1}{1+G_c}$ can be regarded as the system tracking performance to input. $\frac{G_c}{1+G_c}$ represents the system's ability to suppress disturbances. It is characterized by the ability to track low-bandwidth sensor signal at low frequencies and highlight high-bandwidth sensor signals at high frequencies. Therefore, (1) can be rewritten as the following form

$$G_{cl\_fusion} = G_{close} \cdot G_{low} + G_{inhibit} \cdot G_{high} \tag{2}$$

G_{close} and $G_{inhibit}$ represent the tracking and suppression performance of the CLF network structure, respectively.

2.3. Closed-loop Fusion Design

In order to obtain the desired fusion performance, the following two rules should be followed when we design the fusion filter G_c.

$$\omega_{close} << \omega_{low} \tag{3}$$

$$\omega_{inhibit} >> \omega_{high} \tag{4}$$

Based on (3) and (4), The two approximate transformations can be obtained.

$$G_{close} G_{low} \approx G_{close} \tag{5}$$

Preprints (www.preprints.org) | NOT PEER-REVIEWED | Posted: 20 November 2018 doi:10.20944/preprints201811.0497.v1

Peer-reviewed version available at Sensors 2019, 19, 133; doi:10.3390/s19010133

$$G_{inhibit}G_{high} \approx G_{inhibit} \tag{6}$$

where ω_{low}, ω_{high}, ω_{close} and $\omega_{inhibit}$ respectively represent the cutoff frequency of the corresponding transfer characteristic. The numerical simulation of (5) and (6) are shown as Figure 4.

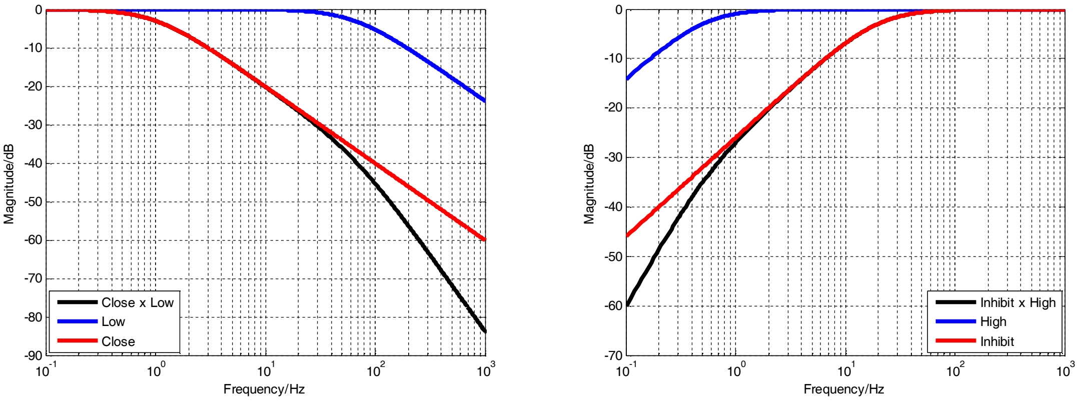

Figure 4. The result of multiplying two transfer functions when cut-off frequency differ greatly

Hence, if the above design requirements has been satisfied, (2) can be approximately reformulated as

$$G_{cl\_fusion} \approx G_{close} + G_{inhibit} \approx 1 \tag{7}$$

As a result, the fusion problem is converted into the design problem of CLF filter. Consider a low-bandwidth sensor as first-order low-pass filter. A high-bandwidth sensor can be expressed as first-order high-pass filter.

$$G_{low}(s) = \frac{\omega_{low}}{s + \omega_{low}} \tag{8}$$

$$G_{high}(s) = \frac{s}{s + \omega_{high}} \tag{9}$$

According to the frequency characteristic of G_{close} and $G_{inhibit}$, we can assume that the closed-loop transfer function of CLF filter is a first-order low-pass filter:

$$G_{close} = \frac{\omega_c}{s + \omega_c} \tag{10}$$

Then the suppression transfer function of CLF filter follows that

$$G_{inhibit} = \frac{s}{s + \omega_c} \tag{11}$$

Thus, the transfer function of CLF is ultimately given by

$$G_{cl\_fusion} = \frac{\omega_c}{s + \omega_c} \cdot \frac{\omega_{low}}{s + \omega_{low}} + \frac{s}{s + \omega_c} \cdot \frac{s}{s + \omega_{high}} \tag{12}$$

In order to achieve the optimal fusion effect, the deviation of $|G_{cl\_fusion}|$ and 1 should be minimized in the desired frequency domain.

According to equations (3) and (4), we can get

Preprints (www.preprints.org) | NOT PEER-REVIEWED | Posted: 20 November 2018 doi:10.20944/preprints201811.0497.v1

Peer-reviewed version available at Sensors 2019, 19, 133; doi:10.3390/s19010133

$$\omega_{high} < \omega_c < \omega_{low} \quad (13)$$

Let k be the fusion ratio, and the value of ω_c can be expressed as

$$\omega_c = \omega_{low} \cdot k + \omega_{high} \cdot (1-k) \qquad k \in [0,1] \quad (14)$$

When $k=0$, we can get $\omega_c = \omega_{high}$, the same can be achieved, if $k=1$, then $\omega_c = \omega_{low}$

Figure 4 shows the errors between the fusion output performance and the desired performance when the fusion ratio k is different. The simulation conditions are $\omega_{low} = 85 \times 2\pi (rad/s)$ and $\omega_{high} = 1.6 \times 2\pi (rad/s)$. The closed-loop characteristics of filter is designed as a first-order low-pass filter. It can be seen that the errors of the fusion output are the smallest when $k = 0.06$ from Figure 5. Therefore, $k = 0.06$ is the optimal fusion ratio. The corresponding cut-off frequency of fusion filter ω_c is $5.196 \times 2\pi (rad/s)$.

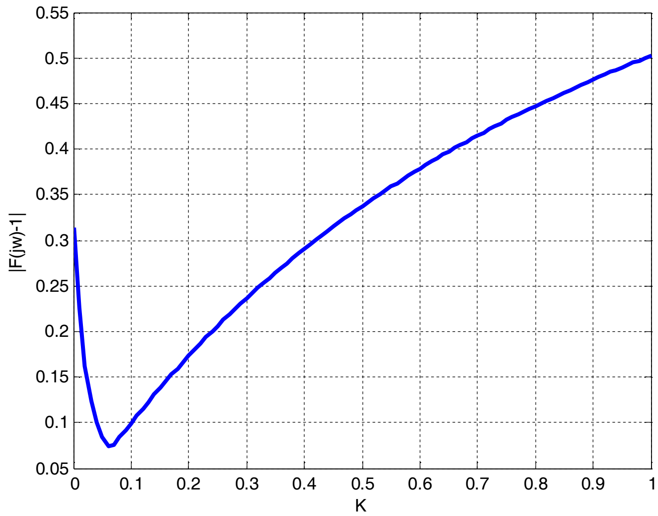

Figure 5. The fusion error of $|G_{cl\_fusion} - 1|$ when k is different

We can find that fusion results are related to transfer function of G_{close} through the above simulation example. In order to analyze the influence of filter order on the fusion effect, the closed-loop characteristic of fusion filter is designed as a second-order or even a third-order low-pass expression. Assuming that the second-order low-pass expression is given by

$$G_{close} = \left(\frac{\omega_c}{s+\omega_c}\right)^2 \quad (14)$$

The third-order low-pass expression can be expressed as

$$G_{close} = \left(\frac{\omega_c}{s+\omega_c}\right)^3 \quad (15)$$

According to aforementioned design steps, the different order G_{close} is used to achieve closed-loop fusion, and different fusion error results are obtained. The second-order low-pass expression is corresponding to the optimal fusion ratio that $k = 0.23$. $k = 0.33$ is the optimal parameter of that third-order low-pass filter is used.

Preprints (www.preprints.org) | NOT PEER-REVIEWED | Posted: 20 November 2018 doi:10.20944/preprints201811.0497.v1

Peer-reviewed version available at Sensors 2019, 19, 133; doi:10.3390/s19010133

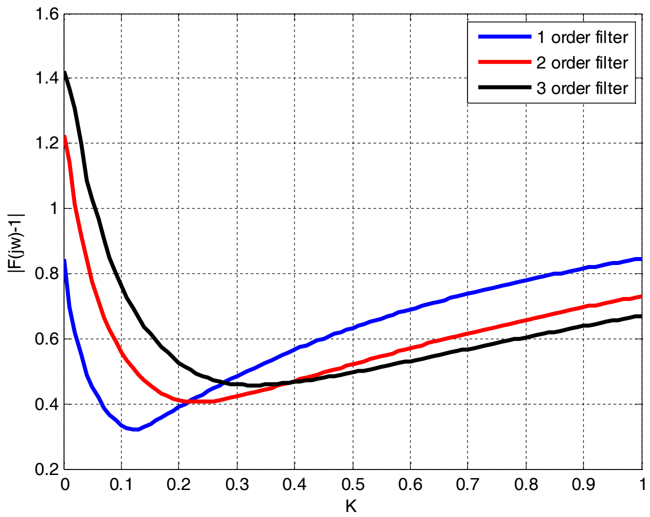

Figure 6. The fusion error of $|G_{cl\_fusion} - 1|$ when the filter order is different

From Figure 6, it can be concluded that the larger the order, the worse fusion precision. Therefore, G_{close} is assumed to be in first-order low-pass form resulting in best fusion accuracy.

3. Fusion Experiment

3.1. Experimental Platform

The inertia sensors fusion experiments are performed to further verify the performance of the proposed CLF methods. The experimental platform, as shown in Figure 7, comprises mirror steering servo system, micro-electro-mechanical system (MEMS) gyroscope and MEMS accelerometers sensors. MEMS inertia sensors are widely used to servo control system due to it's the advantages of smaller, lighter and cheaper. However, ordinary response bandwidth of MEMS gyroscope is not beyond 300 Hz. And MEMS accelerometers have not enough sensitivity to measure low frequency motion, in other words, which have low noise-signal-ratio at low frequency. The open-loop Bode results of mirror steering by using MEMS gyroscope and accelerometers as shown in Figure 8 and Figure 9, respectively.

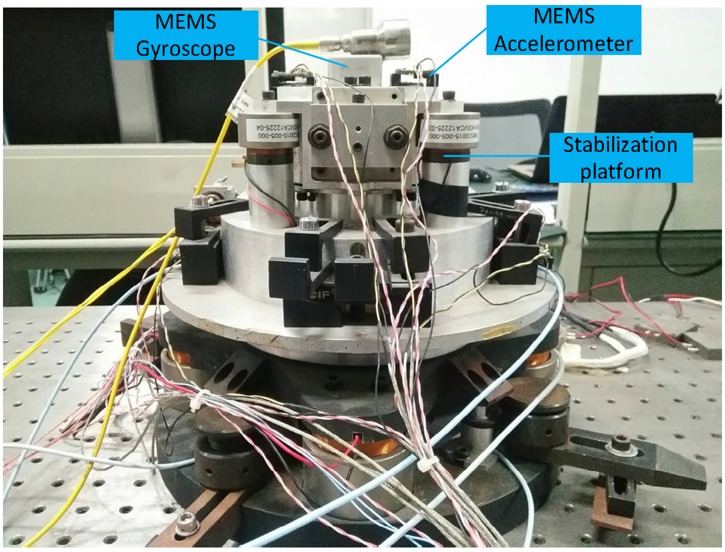

Figure 7. The inertia stable experiment platform

Preprints (www.preprints.org) | NOT PEER-REVIEWED | Posted: 20 November 2018 doi:10.20944/preprints201811.0497.v1

Peer-reviewed version available at *Sensors* **2019**, *19*, 133; doi:10.3390/s19010133

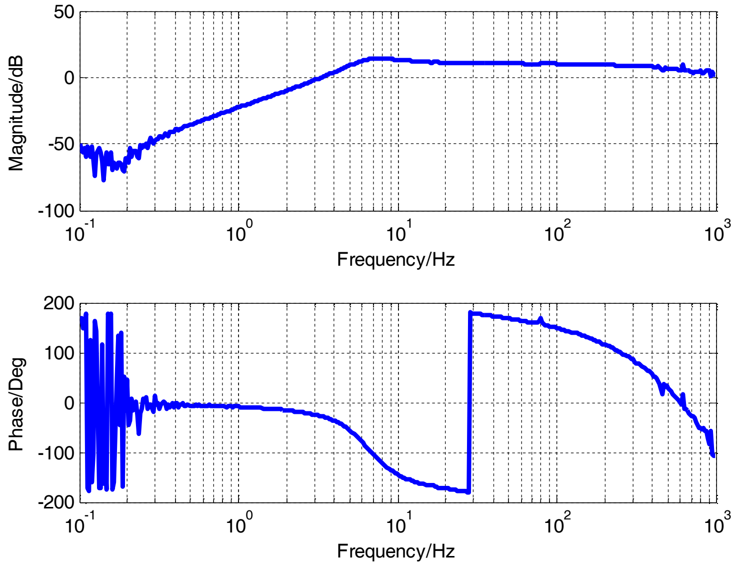

Figure 8. The open-loop Bode with MEMS gyroscope

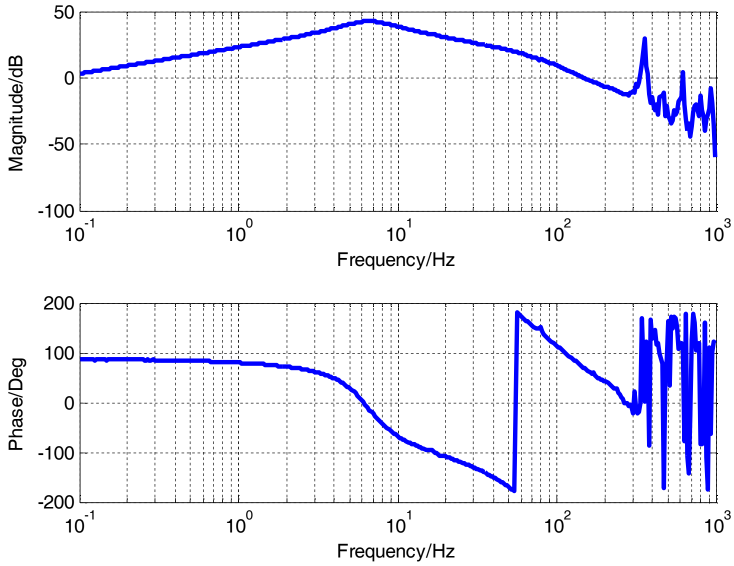

Figure 9. The open-loop Bode with MEMS accelerometers

3.2. Closed-loop Fusion Desgin Based on Velocity Signal

We design a set velocity fusion experiment by utilizing the advantages of MEMS gyroscope and MEMS accelerometers respectively according to Figure 8 and Figure 9. Accelerometers measure angular acceleration signals and gyroscopes measure angular velocities. Compared with position reference signals, one of them is two differential links and the other is one differential link. The sensor frequency feature of gyroscope and accelerometers is measured by PSD, as shown in Figure 10 and Figure 11, respectively. But the high frequency performance of PSD is bad which resulting in the inaccurate result in the high frequency domain. It can be observed that the corresponding frequency point of MEMS gyroscope at -3dB is about 75Hz, and the other is approximately 0.35 Hz for MEMS accelerometers.

Preprints (www.preprints.org) | NOT PEER-REVIEWED | Posted: 20 November 2018 doi:10.20944/preprints201811.0497.v1

Peer-reviewed version available at *Sensors* **2019**, *19*, 133; doi:10.3390/s19010133

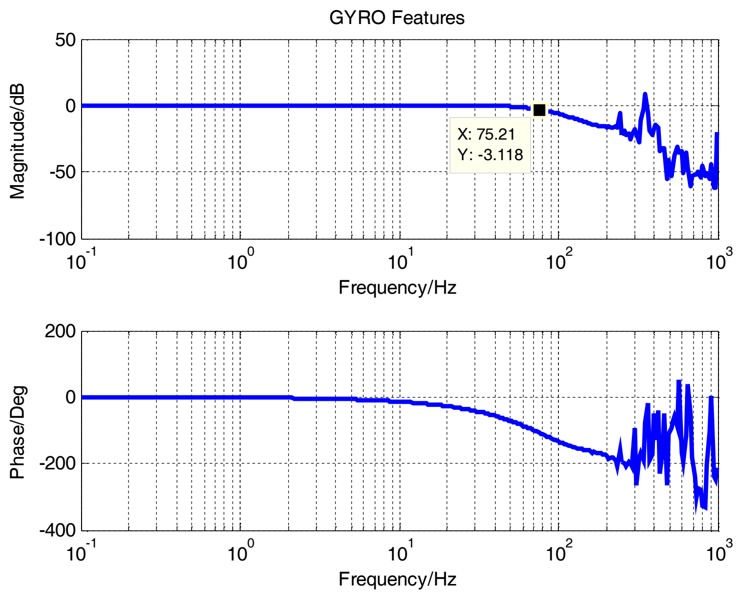

Figure 10. The frequency characteristic of MEMS gyroscope

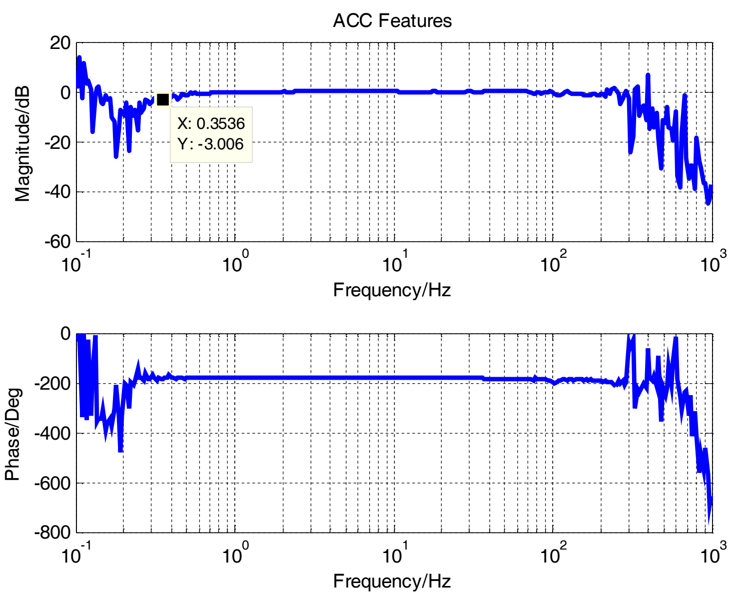

Figure 11. The frequency characteristic of MEMS accelerometers

If the closed-loop transfer function of fusion filter is a first-order filter form. Then $k = 0.88$ and $\omega_c = 248.0793 rad / s$ is obtained from (14). Thus, the closed-loop fusion controller is

$$G_c = \frac{248.0793}{s} \tag{16}$$

3.2. Fusion result with Gyroscope and Accelerometers Based on Velocity signal

Preprints (www.preprints.org) | NOT PEER-REVIEWED | Posted: 20 November 2018 doi:10.20944/preprints201811.0497.v1

Peer-reviewed version available at Sensors 2019, 19, 133; doi:10.3390/s19010133

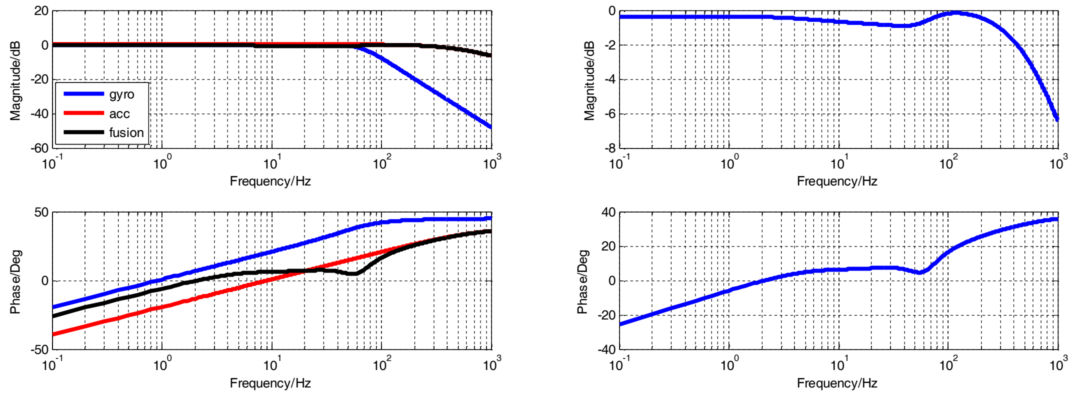

(a) (b)

Figure 12. The simulation result of closed-loop fusion: **(a)** Comparison of characteristics between fusion and low-pass/high-pass sensor; **(b)** Description of fusion result, there is a little fluctuation near 39.483Hz to fusion joint point.

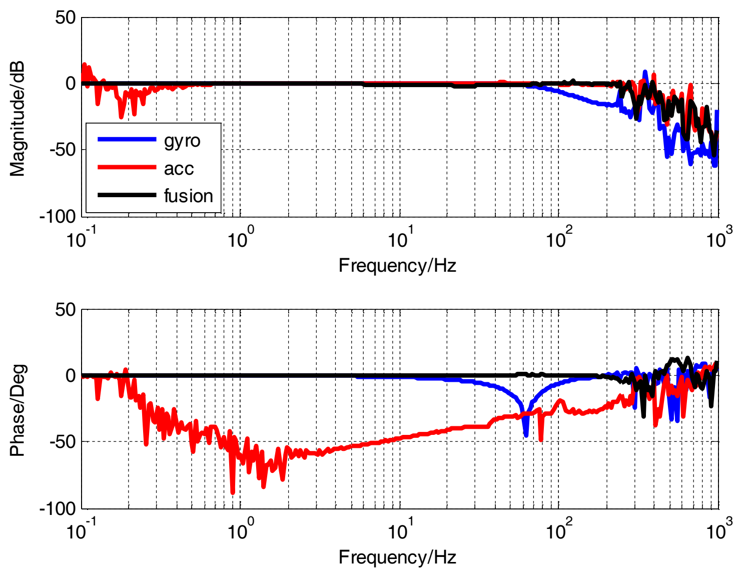

Figure 13. The experiment result of closed-loop fusion

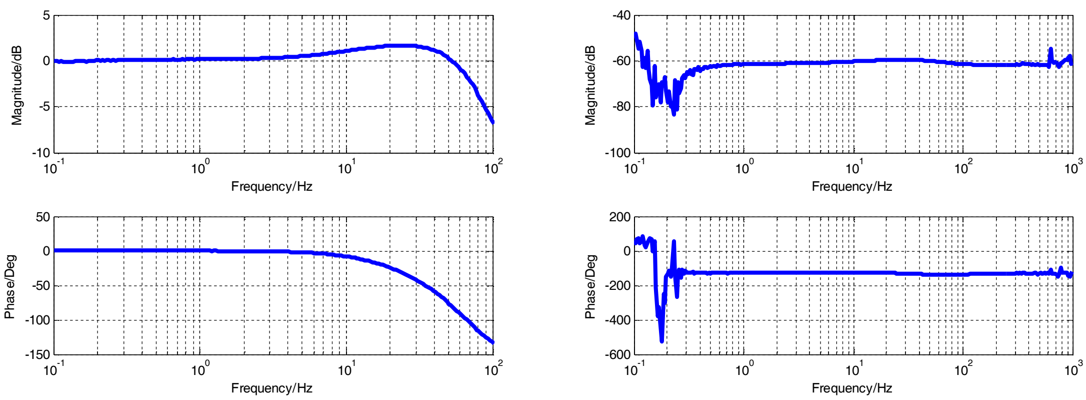

(a) (b)

Figure 14. The experimental fusion error of closed-loop fusion: **(a)** Bode of fusion/gyro; **(b)** Bode of fusion/accelerometers

Preprints (www.preprints.org) | NOT PEER-REVIEWED | Posted: 20 November 2018 doi:10.20944/preprints201811.0497.v1

Peer-reviewed version available at *Sensors* **2019**, *19*, 133; doi:10.3390/s19010133

As we can see in Figure 13, the fusion performance becomes better than any sensor in the whole frequency domain. Specifically, the fusion performance overlapped with MEMS gyroscope performance at low frequencies, and it is the same as MEMS accelerometers at high frequencies. The real measurement fusion errors also demonstrate effectiveness of CLF method as shown in Figure 14. The fusion error is almost zero because of gyro signal at low frequencies in Figure 14(a). High frequency fusion performance is the high frequency characteristic of the accelerometers which resulting in the error at high frequency in Figure 14(b) is pretty small.

4. Conclusions

In this paper, CLF is a high-performance fusion method for multi-sensor fusion technology, which doesn't need to estimate the transfer function of sensors and noise model. But so far, there is little literature to analyze the design of its filters. Therefore, we presented an optimal design of controller of CLF in terms of control theory. As has been shown, the controller design algorithm has proved to be highly fusion performance and ability to eliminate fusion error of frequency joint point effectively. Additionally, we furtherly designed a set velocity fusion experiment with MEMS gyroscope and MEMS accelerometers. The simulation and experiment results showed a satisfactory fusion precision. Therefore, CLF is an ideal fusion method when optimal design method is used.

References

1. Allred, C.J.; Churchill, D.; Buckner, G.D. Real-time estimation of helicopter rotor blade kinematics through measurement of rotation induced acceleration. *Mechanical Systems and Signal Processing* **2017**, *91*, 183-197.
2. Fortino, G.; Ghasemzadeh, H.; Gravina, R.; Liu, P.X.; Poon, C.C.; Wang, Z. Advances in Multi-Sensor Fusion for Body Sensor Networks: Algorithms, Architectures, and Applications: Guest Editorial. Elsevier: 2018.
3. Crassidis, J.L.; Markley, F.L.; Cheng, Y. Survey of nonlinear attitude estimation methods. *Journal of guidance, control, and dynamics* **2007**, *30*, 12-28.
4. Korayem, M.; Yousefzadeh, M.; Kian, S. Precise end-effector pose estimation in spatial cable-driven parallel robots with elastic cables using a data fusion method. *Measurement* **2018**, *130*, 177-190.
5. Jiang, Y.-h.; Zhang, G.; Tang, X.; Li, D.; Huang, W.-c. Detection and correction of relative attitude errors for ZY1-02C. *IEEE Transactions on Geoscience and Remote Sensing* **2014**, *52*, 7674-7683.
6. Iwata, T. Precision attitude and position determination for the Advanced Land Observing Satellite (ALOS). In Proceedings of Enabling Sensor and Platform Technologies for Spaceborne Remote Sensing; pp. 34-51.
7. Iwata, T.; Kawahara, T.; Muranaka, N.; Laughlin, D. High-bandwidth attitude determination using jitter measurements and optimal filtering. In Proceedings of AIAA Guidance, Navigation, and Control Conference; p. 6311.
8. Murrell, J. Precision attitude determination for multimission spacecraft. In Proceedings of Guidance and Control Conference; p. 1248.
9. Algrain, M.C.; Powers, R.M. Line-of-sight pointing accuracy/stability analysis and computer simulation for small spacecraft. In Proceedings of Acquisition, Tracking, and Pointing X; pp. 62-77.
10. Ma, J.; Sun, S. Information fusion estimators for systems with multiple sensors of different packet dropout rates. *Information Fusion* **2011**, *12*, 213-222.
11. Saadi, I.; Farooq, B.; Mustafa, A.; Teller, J.; Cools, M. An efficient hierarchical model for multi-source information fusion. *Expert Systems with Applications* **2018**.

Preprints (www.preprints.org) | NOT PEER-REVIEWED | Posted: 20 November 2018 doi:10.20944/preprints201811.0497.v1

Peer-reviewed version available at *Sensors* **2019**, *19*, 133; doi:10.3390/s19010133

12. Benini, A.; Senatore, R.; D'Angelo, F.; Orsini, D.; Quatraro, E.; Verola, M.; Pizzarulli, A. A closed-loop procedure for the modeling and tuning of Kalman Filter for FOG INS. In Proceedings of Inertial Sensors and Systems Symposium (ISS), 2015 DGON; pp. 1-19.
13. Marins, J.L.; Yun, X.; Bachmann, E.R.; McGhee, R.B.; Zyda, M.J. An extended Kalman filter for quaternion-based orientation estimation using MARG sensors. In Proceedings of Intelligent Robots and Systems, 2001. Proceedings. 2001 IEEE/RSJ International Conference on; pp. 2003-2011.
14. Sasiadek, J.; Hartana, P. Sensor data fusion using Kalman filter. In Proceedings of Proceedings of the Third International Conference on Information Fusion; pp. 19-25.
15. Odry, Á.; Fullér, R.; Rudas, I.J.; Odry, P. Kalman filter for mobile-robot attitude estimation: Novel optimized and adaptive solutions. *Mechanical Systems and Signal Processing* **2018**, *110*, 569-589.
16. Algrain, M.C. Gyroless line-of-sight stabilization for pointing and tracking systems. *Optical engineering* **1994**, *33*, 1255-1261.
17. Ji, Y.; Xu, M.; Li, X.; Wu, T.; Tuo, W.; Wu, J.; Dong, J. Error Analysis of Magnetohydrodynamic Angular Rate Sensor Combing with Coriolis Effect at Low Frequency. *Sensors* **2018**, *18*, 1921.
18. Ji, Y.; Li, X.; Wu, T.; Chen, C. Theoretical and experimental study of radial velocity generation for extending bandwidth of magnetohydrodynamic angular rate sensor at low frequency. *Sensors* **2015**, *15*, 31606-31619.
19. Algrain, M.C.; Powers, R.M.; Woehrer, M.K. Extended-bandwidth spacecraft attitude determination using gyros and linear accelerometers. In Proceedings of Optical Spectroscopic Techniques and Instrumentation for Atmospheric and Space Research II; pp. 306-319.